

# *Considering the effect of graphene loading in water-based epoxy coatings*

**T. Monetta, A. Acquesta, A. Carangelo &  
F. Bellucci**

**Journal of Coatings Technology and  
Research**

ISSN 1547-0091

J Coat Technol Res

DOI 10.1007/s11998-018-0045-8



**Your article is protected by copyright and all rights are held exclusively by American Coatings Association. This e-offprint is for personal use only and shall not be self-archived in electronic repositories. If you wish to self-archive your article, please use the accepted manuscript version for posting on your own website. You may further deposit the accepted manuscript version in any repository, provided it is only made publicly available 12 months after official publication or later and provided acknowledgement is given to the original source of publication and a link is inserted to the published article on Springer's website. The link must be accompanied by the following text: "The final publication is available at [link.springer.com](http://link.springer.com)".**

# Considering the effect of graphene loading in water-based epoxy coatings

T. Monetta , A. Acquesta, A. Carangelo, F. Bellucci

© American Coatings Association 2018

**Abstract** Recently, graphene has gained increasing interest in numerous fields of application and, in particular, it has been used as a nanofiller in the preparation of polymeric composites to improve their mechanical and transport properties. However, the effect of graphene as a potential additive for anticorrosive organic coatings is not widely studied. In this work, low levels of graphene nanosheets, 0.5 and 1 wt%, were added to an additive-free waterborne epoxy resin applied to Al2024-T3 aluminum alloy samples. The presence of graphene did not affect the polymerization process of the resin and the adhesion at coating/substrate interface, as demonstrated by experimental results, while showing a slight effect on coatings wettability. Electrochemical analysis revealed an improvement of the protective properties of the coating that could be assigned to a slow absorption rate of the electrolytes in the polymeric matrix and a lesser amount of absorbed water than the unloaded film.

**Keywords** Coatings, Graphene, Nanocomposite, Corrosion, Epoxy water-based resin

## Introduction

The graphene used as nanofiller in polymer matrices to form advanced multifunctional materials has drawn increasing attention in various areas of application.<sup>1-4</sup> The graphene incorporated in polymeric materials can lead to a significant increase in the electrical (as conductivity) and thermal properties (as cure kinet-

ics)<sup>5-8</sup> and an improvement in the mechanical properties of nanocomposites.<sup>9-11</sup> In the meantime, few papers<sup>12-17</sup> concerning the development of nanocomposites address the increase in the protective properties of organic coatings. Reports on epoxy/graphene coatings are still less frequent.<sup>14,18-20</sup> Moreover, few papers describe the use of waterborne resins<sup>15,21-24</sup> even if, the environmentally friendly solutions that take into account the new regulations about the emission of volatile organic compounds<sup>25-28</sup> are now of significant interest. Aluminum needs to be protected to reduce its corrosion rate to improve the substrate durability. Due to its active/passive behavior, it is sensitive to the presence of chloride ions when in contact with its surface. Several types of eco-friendly surface treatments, or coating systems, have been investigated to decrease the aluminum corrosion rate when exposed to an environment containing chloride ions.<sup>28-36</sup> The aim of this paper is to evaluate the effect of graphene on protective properties of coatings, obtained by incorporating low levels of graphene, i.e., 0.5 and 1 wt%, into the waterborne epoxy resin and applied to Al2024-T3 aluminum alloys samples. Differential scanning calorimetry technique (DSC) has been performed to study the influence of the nanofiller on the epoxy matrix, while the adhesion at coating/substrate interface was assessed using the tape test. The wettability of coatings has been studied through the water contact angle analysis (WCA). The anticorrosive properties were investigated by using electrochemical impedance spectroscopy tests (EIS) to evaluate the coating impedance and capacitance as a function of time when in contact with an aggressive aqueous solution.

## Experimental

Graphene nanosheets, bought from Cometox (Italy), present a width less than 2  $\mu\text{m}$  and an average

---

T. Monetta (✉), A. Acquesta, A. Carangelo,  
F. Bellucci  
Department of Chemical Engineering, Materials and  
Industrial Production, University of Napoli Federico II,  
Piazzale Tecchio 80, 80125 Naples, Italy  
e-mail: monetta@unina.it

thickness of about 2 nm. The epoxy system (Wapex 660, Sikkens, Italy) is a bicomponent commercial waterborne resin, without corrosion inhibitors. The epoxy resin and the hardener were mixed in the proportional mass indicated by the manufacturer. The chemical compounds of the resin components are listed in Table 1.

Before painting, the Al2024-T3 substrates, having dimensions 20 cm × 10 cm × 0.5 cm, were degreased by acetone and dried by using compressed air.

The amounts of nanofiller chosen to investigate the influence of the dispersed graphene in the polymer matrix were 0.5 and 1 wt%. The nomenclature used to indicate the samples is reported in Table 2.

### Coating preparation

Graphene nanosheets were dispersed in component A of the coating using an ultrasonic bath (frequency of 50 Hz) for 20 min. The curing agent was added to the graphene/epoxy blend, and the latter was mixed further for 20 min using a mechanical stirrer. Finally, the coating was spread on the aluminum substrates using a spiral bar applicator and oven-cured at 150°C for 10 min, recording a dry thickness of  $27 \pm 1.3 \mu\text{m}$ , measured with an Elcometer Dualscope MP0R-Fp (IMCD Italia Spa, Italy).

### Methods

The thermal analysis was performed to evaluate the effect of the nanofiller on the epoxy matrix properties. Three scans (first heating, then cooling and heating again) were carried out from 30 to 250°C at heating rate of  $10^\circ\text{C min}^{-1}$ . The measurement was taken in a dry nitrogen atmosphere by using a Mettler Toledo DSC12E (Mettler-Toledo Spa, Italy) apparatus. The interfacial adhesion between the coating and the aluminum sheet was analyzed by tape test with a standard blade (Sheen Instruments, Italy), according to ASTM D3359-09. Wettability of the cured coating was investigated by measuring the water contact angle (WCA) using an OCA 15EC (DataPhysics Instruments GmbH, Germany). Water droplets (3.5  $\mu\text{L}$  each) were dispensed on the surface of specimens, and the WCA

was evaluated by performing 50 measurements taken at different points on the surface. Electrochemical impedance spectroscopy tests (EIS) were carried out to characterize the protective properties of the coatings, following ISO 16773-2016. A standard electrochemical cell, containing a saturated calomel reference electrode (SCE), platinum counter electrode and the coated aluminum sample as working electrode, was used. The apparatus used to perform the electrochemical test consisted of the frequency response analyzer 1255 Solartron, and the potentiostat/galvanostat, 1286 Solartron (Photo Analytical Srl, Italy). The tests were carried out in an air saturated 3.5 wt% NaCl aqueous solution for 21 days, exposing an area of about 5 cm<sup>2</sup>. The frequency range varied from 10<sup>5</sup> Hz to 0.02 Hz. Measurements were taken at open-circuit potential (OCP) applying an amplitude sinusoidal voltage of 40 mV. All measurements were taken at room temperature and repeated at least three times to ensure reproducibility and accuracy.

### Results and discussion

DSC measurements (Fig. 1) were taken on the EP and the epoxy-graphene samples. For clarity, only the third scan for each sample is reported. Due to the raw material complex composition (a commercial product), the study and interpretation of DSC spectra are quite difficult, so the experimental results obtained have been used only for a preliminary characterization of cured coatings. Data seem to indicate that the epoxy matrix physical properties (if evaluated through glass transition temperature, specific heat capacity, etc.) are not affected by the graphene loading. Therefore, the effect of nanosheets on the protective behavior of the coating, as will be discussed in the subsequent para-

**Table 2: Abbreviation used to indicate the tested specimens**

Sample	Nomenclature
Unfilled coating	EP
Coating containing 0.5 wt% of graphene	EG05
Coating containing 1 wt% of graphene	EG1

**Table 1: Chemical composition of waterborne epoxy resin**

	Common names	CAS number	Wt%	Acronyms
Component A	Adduct resin epoxy-polyamine tetraethylenepentamine	112-57-2	≥ 10, < 20	TEPA
	Bisphenol A-co-epichlorohydrin	25068-38-6	≥ 0.25, < 1	DGEBA
	Bisphenol-F epichlorohydrin	28064-14-4	≥ 0.25	DGEBF
Component B	Bisphenol A-co-epichlorohydrin	25068-38-6	≥ 50, < 75	DGEBA
	Bisphenol-F epichlorohydrin	28064-14-4	≥ 20, < 25	DGEBF
	2,3-Epoxypropyl neodecanoate	26761-45-5	≥ 2.5, < 25	

graph, should be attributed neither to a physical modification of epoxy matrix nor a curing process.

When a film is used to protect a metallic substrate, good adhesion to substrate is needed. Poor adhesion, in

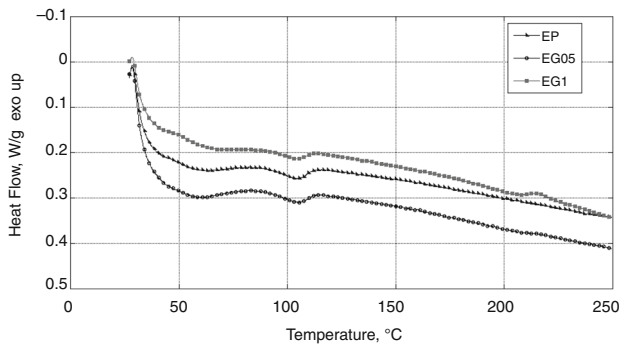


**Fig. 1:** Thermal analysis of the filled and unfilled samples

fact, permits electrolytes to accumulate at film/substrate interface triggering the degradation process.<sup>37</sup> Therefore, a good adhesion delays the delamination of coating when the corrosion starts. Thus, tape tests (Figs. 2, 3, and 4) highlighted that the interface adhesion of nanocoating/aluminum system was not influenced by the presence of graphene nanosheets. According to the ASTM standard, all samples received a score of 4B (less than 5% peeling).

Water contact angle measurements were taken to study the influence of graphene on the wettability of coating (Fig. 5; Table 3).

The value of contact angle increased from 65.1° (recorded for the unfilled epoxy coating) to 71.3° (EG05 sample) to 81.2° (EG1 sample). This rise seems to be linked to the quantity of nanofiller contained in the resin; in fact, the contact angle increased as more filler was added, conferring to the surface a slightly lower wettability.

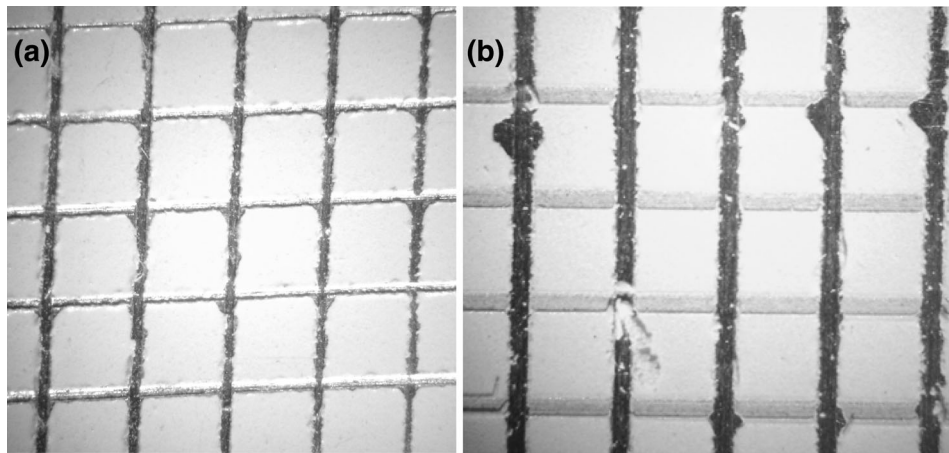


**Fig. 2:** A picture of the EP sample (a) before and (b) after the tape test

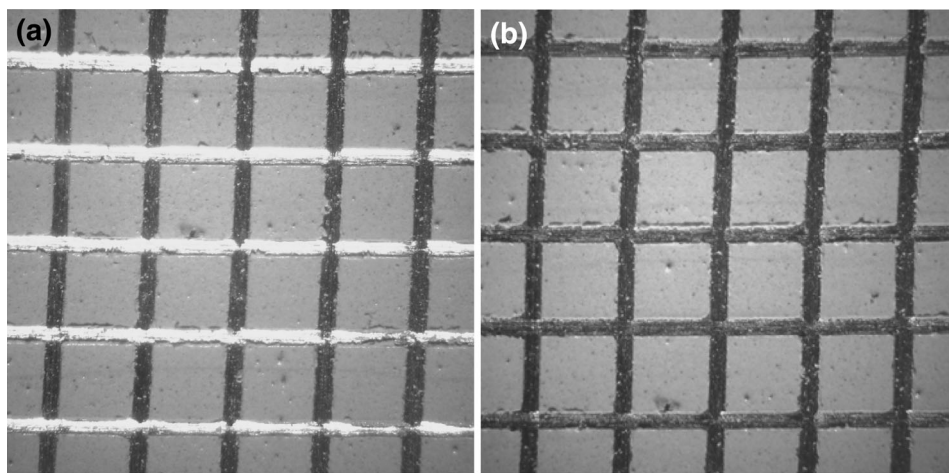


**Fig. 3:** A picture of the EG05 sample (a) before and (b) after the tape test

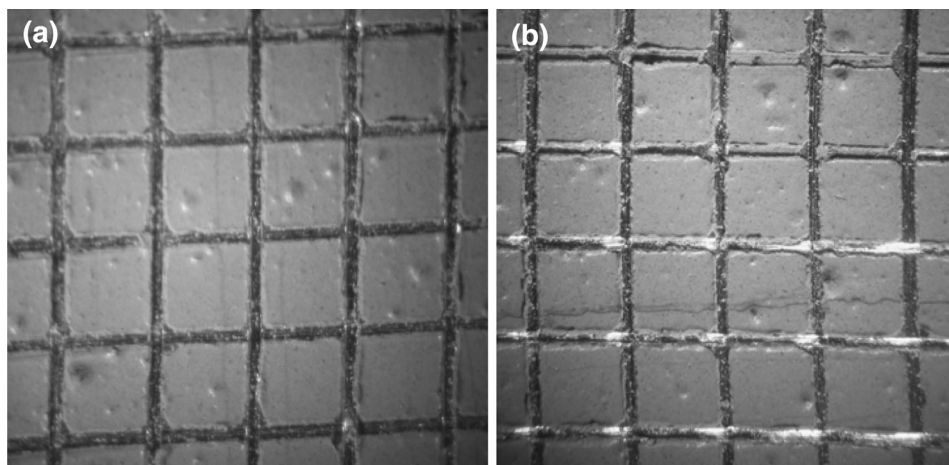


Fig. 4: A picture of the EG1 sample (a) before and (b) after the tape test

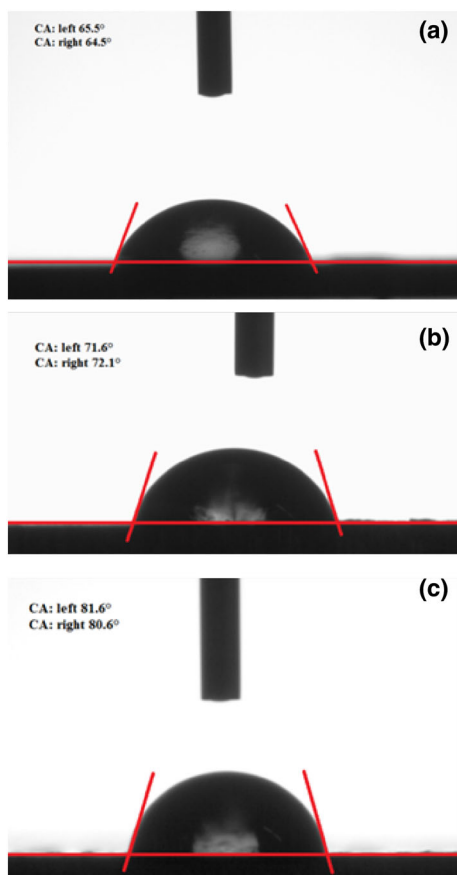


Fig. 5: Water contact angle pictures of (a) unfilled coating, EP, (b) epoxy-graphene coating with 0.5 wt% of nanofiller, EG05 and (c) epoxy-graphene coating with 1 wt% of nanofiller, EG1

The electrochemical properties of coatings were monitored by EIS tests during 21 days of exposure to an aerated 3.5 wt% NaCl aqueous solution. Acquired results are reported in Figs. 6, 7, and 8.

Table 3: Average values of water contact angles of specimens

Sample	EP	EG05	EG1
Water contact angle (°)	65.1	71.3	81.2

As shown in data reported in Fig. 6a, the unloaded epoxy coating offered poor corrosion. In fact, the value of low-frequency impedance modulus (attributed to the coating resistance) was slightly less than  $10^7 \Omega \text{ cm}^2$ , after only one day of exposure to the test solution. Coatings are considered of poor quality when the impedance modulus value is lower than  $10^7 \Omega \text{ cm}^2$ . The result highlighted the weak anticorrosive properties of the material, caused by the lack of useful pigments, allowing the water and the electrolytes rapid penetration into the coating. After 4 days of immersion, the impedance modulus at low frequency decreased to about  $4 \times 10^6 \Omega \text{ cm}^2$ , while it was possible to detect the development of corrosion phenomena at the coating/metallic interface. This finding, increasingly evident along with exposure time, was caused by the absorption of water and electrolytes through the film with the more visible development of anodic area at the metallic substrates.<sup>38</sup> For prolonged immersion time (21 days) and at very low frequency ( $10^{-2}$  Hz), the impedance modulus increased. This effect can be assigned to the formation of corrosion products at the interface which filled the pores of the coating increasing the overall resistance.

The impedance results are confirmed by the phase angle plot that emphasizes these effects.<sup>38</sup> In fact, after one day of exposure to the test solution, the phase angle (Fig. 6b) showed a value of about  $80^\circ$  at high frequency, while a minimum value of  $3^\circ$  has been observed at a frequency of about 0.25 Hz. Moreover, it was possible to observe an increase in the phase angle at the lowest frequency range ( $10^{-2}$ – $10^0$  Hz). The rise

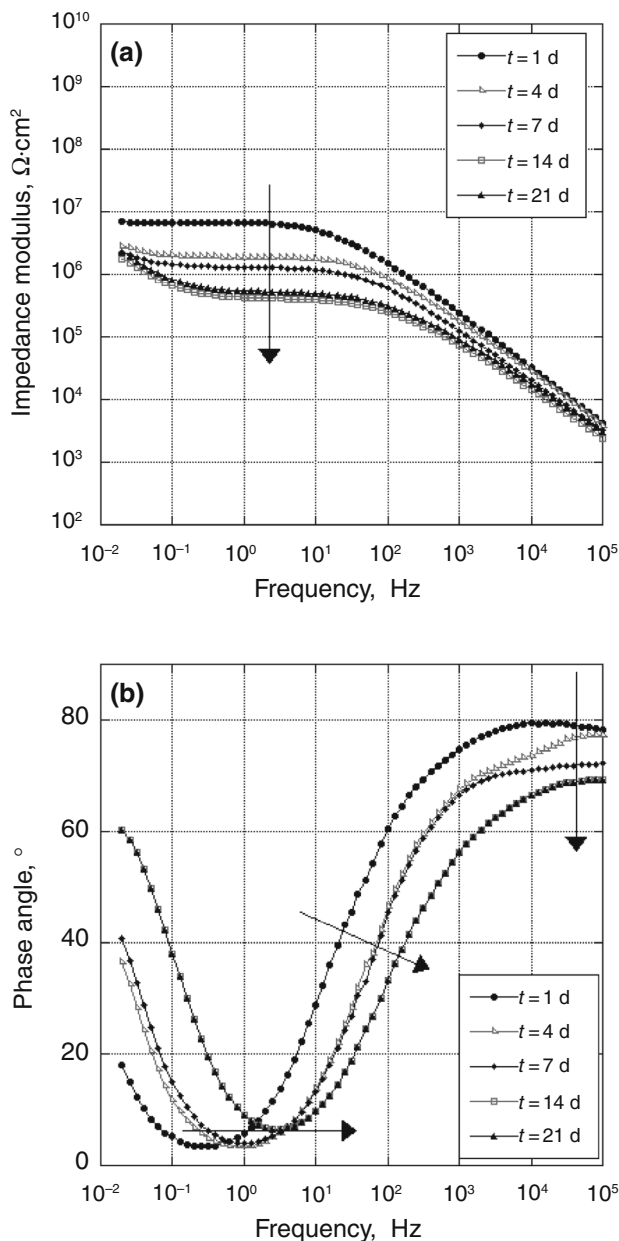


Fig. 6: Bode plots, (a) modulus and (b) phase angle, of the unfilled coating (EP) in the test solution

suggested that the corrosion process at the alloy/coating interface was started. Therefore, it can be assumed that the solution, penetrating the coating in the 24 h of exposure, has reached the metallic substrate and has activated corrosion phenomena.<sup>38</sup> The phase angle minimum shifted toward the high frequencies, as the immersion time elapsed, confirming the further degradation of the coating. On the other hand, the broad variation of the phase angle, recorded in the medium-high frequency range, suggested an increase in corrosion products formation, showing the continuous evolution of metallic substrate degradation.

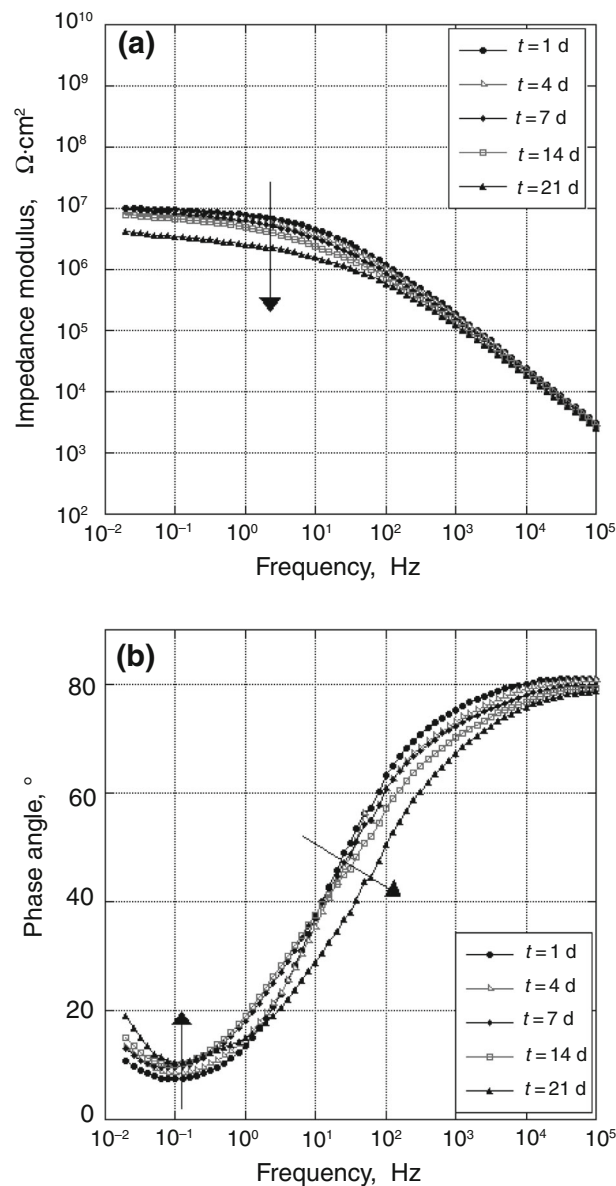
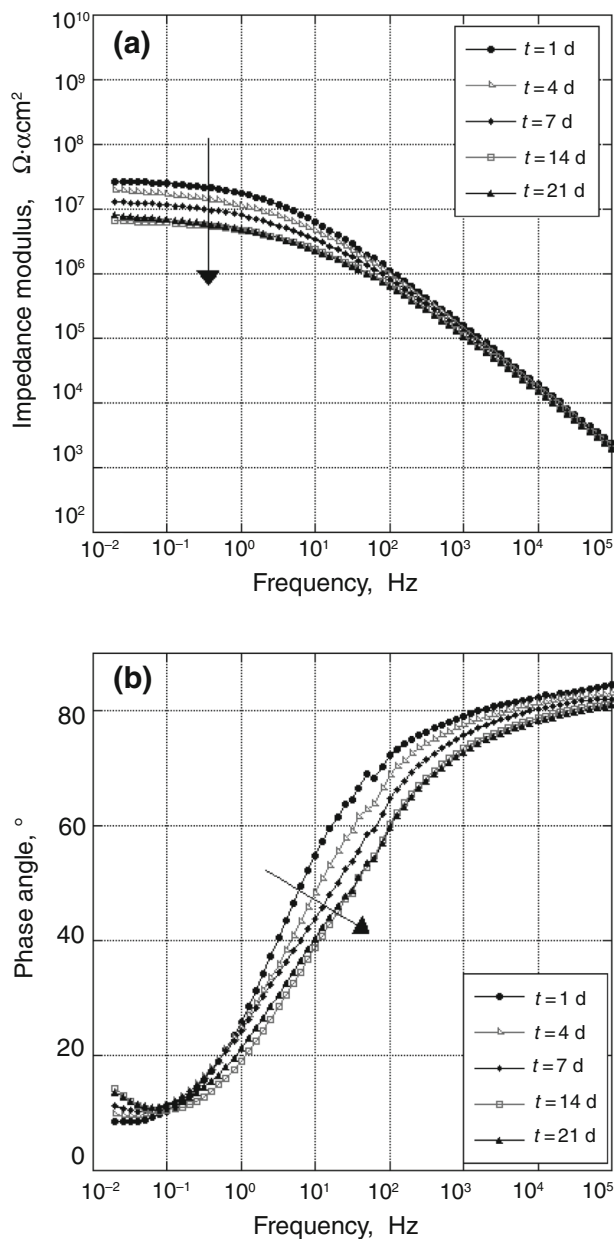


Fig. 7: Bode plots, (a) modulus and (b) phase angle, of epoxy-graphene coating loaded with 0.5 wt% (EG05) of graphene nanofiller in the test solution

In Fig. 7, Bode plots of the EG05 specimen are reported. The behavior observed is quite different compared to the EP sample. A very slight decrease in the impedance modulus values (Fig. 7a) in time has been observed, suggesting an improved stability of the loaded epoxy coating. Moreover, after one day of immersion in the aggressive solution, EG05 specimen showed a higher impedance modulus value compared to that displayed by EP sample, indicating enhanced protective properties of the coating. The low-frequency impedance modulus lightly dropped with increasing the immersion time in the test solution up to 21 days.



**Fig. 8: Bode plots, (a) modulus and (b) phase angle, of epoxy-graphene coating loaded with 1 wt% (EG1) of graphene nanofiller in the test solution**

In this case, no increase in the impedance modulus at very low frequencies ( $10^{-2}$  Hz) was detected in the time interval of 14–21 days, unlike the unfilled coating, EP. Hence, the EIS response of the epoxy loaded coating is improved by the addition of 0.5 wt% of graphene.

Looking at the phase angle data in Fig. 7b, the benefit offered by the presence of graphene on the stability of the loaded epoxy coating is evident. After one day of exposure, the phase angle plot showed a value of about  $80^\circ$  at high frequency, while a minimum value was observed at a frequency of about 0.1 Hz. Furthermore,

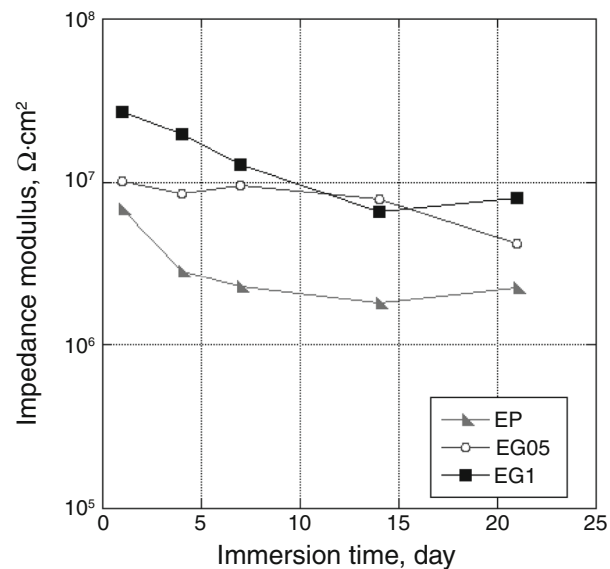


**Fig. 9: Evolution of impedance modulus values at 0.02 Hz of EP sample (triangular dots), EG05 sample (circle dots) and EG1 sample (square dots)**

the rise of the phase angle recorded at the lowest frequency range ( $10^{-1}$ – $10^{-2}$  Hz) was much less pronounced if compared with the data obtained for unfilled coating. This trend suggested that there was limited initiation of the corrosion process at the alloy/coating interface. It is also worthy of mention that the phase angle shifted toward the low-frequency range in the time interval of 1–7 days. These findings can be related to the corrosion products, present at the interface, which filled the coating porosity, leading to a more compact coating.<sup>37</sup> After 14 days, the deterioration of the coating became evident as indicated by the shift of the phase angle plot toward the high frequencies. Also these results support the hypothesis that the loaded epoxy coating appears more stable than the unfilled sample during the exposure time, even if the electrolyte completely penetrates the coating upon one day of immersion.

The impedance modulus of EG1 sample (Fig. 8a) showed, after the first 24 h of immersion in the solution test, a value of about  $6 \times 10^7 \Omega \text{ cm}^2$ , the highest measured in this test campaign. In the rest of immersion time, the impedance modulus slightly decreased showing values always above  $10^7 \Omega \text{ cm}^2$  in the range of low frequencies. An examination of the phase angle plot revealed further beneficial effects. In fact, the curves did not clearly show a minimum at very low frequency until 4 days of immersion, as observed in the EP and EG05 samples. Consequently, no corrosion phenomena can be detected in the above time interval, revealing a higher barrier effect of the loaded coating. The phase angle showed a slight tendency to increase in the time interval 4–7 days of immersion time. After 14 days, a minimum has been recorded at the lowest frequencies, suggesting that the corrosion process at the metallic interface started to develop. Also in this case, phase



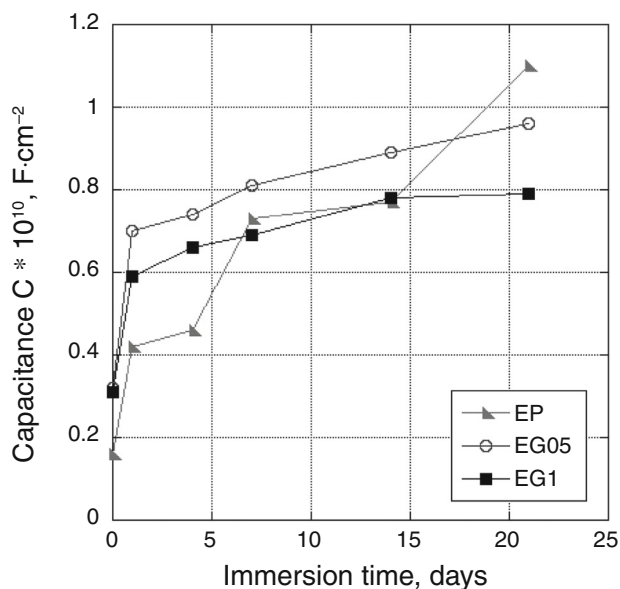


**Fig. 10: Evolution of coating capacitance of EP sample (triangular dots), EG05 sample (circle dots), and EG1 sample (square dots)**

angle data were shifted toward lower frequencies due to improved coating protective properties.

Impedance modulus values, evaluated at 0.02 Hz, are shown in Fig. 9, and an immediate comparison between them can be made. As can be seen, filled coatings exhibit impedance modulus values higher than the unfilled one for all exposure times.

Capacitance value, assumed by organic coating when exposed to a water solution, is a useful parameter to monitor water uptake in coatings.<sup>39,40</sup> It can be calculated by using equation (1)<sup>41</sup>:

$$C = \frac{1}{(2\pi f_i Z_i)} = \frac{1}{(2\pi f Z'')} \quad (1)$$

here  $f_i$  (equal to 6.5 kHz) is a frequency value where the slope of the impedance modulus curve is equal to  $-1$  and  $Z_i$  is the imaginary part (or reactive component) of the impedance. The results, reported in Fig. 10, show the difference in behavior between coatings loaded with different amounts of graphene.

Capacitance values were recorded, as a first approximation, assuming that the swelling of the coating due to water absorption could be neglected, thus the area and thickness of coating do not change and the coating can be considered as an ideal medium. As can be seen at the beginning of the analysis campaign, *i.e.*, when the test starts and it is possible to consider that the coatings are dry, capacitance values were  $1.6 \times 10^{10}$ ,  $3.2 \times 10^{10}$  and  $3.1 \times 10^{10}$  F cm<sup>-2</sup> for EP, EG05 and EG1 samples, respectively, indicating a distinct nature of the coatings. In order to assess the consistency of capacitance data, the relative permittivity ( $\epsilon$ ) of materials has been considered. The  $\epsilon$  has been calculated from capacitance values obtained by applying equation (2). The  $\epsilon$  value

for EP sample was 4.93, in agreement with Ku and Liepins.<sup>42</sup> In contrast, coatings filled with 0.5 and 1 wt% of graphene (EG05 and EG1) presented  $\epsilon$  values of 10.21 and 9.70, respectively, and as a matter of fact the conductivity of the graphene nanofillers did increase the permittivity of the unfilled coating, due to the polarizing effect of graphene.

$$C = \epsilon_0 \epsilon_r A/d \quad (2)$$

where  $C$  is the capacitance of flat, parallel metallic plates of area  $A$  and separation  $d$ ,  $\epsilon_0$  is the vacuum permittivity, equal to  $8.85 \times 10^{-12}$  F·m<sup>-1</sup> and  $\epsilon_r$  is the relative permittivity of the dielectric material between the plates.

Literature review reveals that increased performances of organic coatings are attributed to the barrier effect<sup>43,44</sup> played by graphene that induces a water diffusivity decrease through the coating. In other words, the effect of graphene seems to be due, simply, to an increase in tortuosity of diffusion pathway of water through the coating. Data reported in Fig. 10 showed that the coatings exhibited different capacitance trends with time. Namely, the net epoxy coating, after a fast increase in the capacitance coating at the beginning of the test, displayed a quasi-steady-state plateau and a subsequent step rise. While nanocomposite coatings, at the beginning of the measurement, showed a fast increase in the capacitance coating, they progressively slowed down until a saturation stage was reached. This trend indicates a different water absorption process. The equations of straight line interpolation of experimental data, evaluated excluding the first experimental value, are  $y = 0.00131x + 0.6957$  ( $R^2 = 0.97$ ) and  $y = 0.0095x + 0.6132$  ( $R^2 = 0.90$ ), for EG1 and EG05 samples, respectively. Their slopes are equal to  $0.75^\circ$  (for EG05 sample) and  $0.54^\circ$  (for EG1 sample), confirming the steady-state reaching for both samples. In conclusion: the samples EG05 and EG1 have been saturated by water in 1 day, while the EP sample continued to adsorb the electrolyte until the end of experiments. This occurrence seems to contradict the experimental evidence, reported in several papers, that demonstrates a reduction of material flow when the resin is added with graphene, while it can be explained considering that the total amount of water uptaken is reduced. In other words, coating permeability is reduced both for the decrease in diffusivity and solubility of water due to the extended pathway and to the hydrophobic character of graphene. Thus, it is possible to suppose that, due to graphene loading, a fraction of free volumes inside the coating are not available to water, reducing the total amount of water uptake, even if this assumption needs to be verified collecting more data.

## Conclusions

The influence of graphene nanosheets, incorporated in a water-based epoxy coating and applied to Al2024T3 samples, has been evaluated. The results showed that:

- resin (1) structural properties and (2) adhesion to the substrate were not affected by the presence of graphene;
- nanosheets addition conferred some hydrophobic character to the coating;
- loaded coatings showed improved electrochemical performances toward corrosion.

Based on the experimental results, it can be supposed that the change of the electrochemical and physical behavior of the coatings is not merely related to a physical effect. It may be due to some filler-matrix interaction, due to polarizing effect of graphene and to its hydrophobic character, that has not been evidenced previously and which deserves further studies.

## References

1. Kumar, S, Raj, S, Jain, S, Chatterjee, K, "Multifunctional Biodegradable Polymer Nanocomposite Incorporating Graphene-Silver Hybrid for Biomedical Applications." *Mater. Des.*, **108** 319–332 (2016)
2. Ladani, RB, Wu, S, Kinloch, AJ, Ghorbani, K, Zhang, J, Mouritz, AP, Wang, CH, "Multifunctional Properties of Epoxy Nanocomposites Reinforced by Aligned Nanoscale Carbon." *Mater. Des.*, **94** 554–564 (2016)
3. Wang, C, Lan, Y, Yu, W, Li, X, Qian, Y, Liu, H, "Preparation of Amino-Functionalized Graphene Oxide/Polyimide Composite Films with Improved Mechanical, Thermal and Hydrophobic Properties." *Appl. Surf. Sci.*, **362** 11–19 (2016)
4. Zhao, S, Chang, H, Chen, S, Cui, J, Yan, Y, "High-Performance and Multifunctional Epoxy Composites Filled with Epoxide-Functionalized Graphene." *Eur. Polym. J.*, **84** 300–312 (2016)
5. Kim, H, Miura, Y, Macosko, CW, "Graphene/Polyurethane Nanocomposites for Improved Gas Barrier and Electrical Conductivity." *Chem. Mater.*, **22** 3441–3450 (2010)
6. Song, SH, Park, KH, Kim, BH, Choi, YW, Jun, GH, Lee, DJ, Kong, BS, Paik, KW, Jeon, S, "Enhanced Thermal Conductivity of Epoxy-Graphene Composites by Using Non-Oxidized Graphene Flakes with Non-Covalent Functionalization." *Adv. Mater.*, **25** 732–737 (2013)
7. Tang, B, Hu, G, Gao, H, Hai, L, "Application of Graphene as Filler to Improve Thermal Transport Property of Epoxy Resin for Thermal Interface Materials." *Int. J. Heat Mass Transf.*, **85** 420–429 (2015)
8. Wang, Y, Yu, J, Dai, W, Song, Y, Wang, D, Zeng, L, Jiang, N, "Enhanced Thermal and Electrical Properties of Epoxy Composites Reinforced with Graphene Nanoplatelets." *Polym. Compos.*, **36** 556–565 (2015)
9. Wajid, AS, Ahmed, HST, Das, S, Irin, F, Jankowski, AF, Green, MJ, "High-Performance Pristine Graphene/Epoxy Composites with Enhanced Mechanical and Electrical Properties." *Macromol. Mater. Eng.*, **298** 339–347 (2013)
10. Wang, F, Drzal, LT, Qin, Y, Huang, Z, "Mechanical Properties and Thermal Conductivity of Graphene Nanoplatelet/Epoxy Composites." *J. Mater. Sci.*, **50** 1082–1093 (2015)
11. Zhang, B, Asmatulu, R, Soltani, SA, Le, LN, Kumar, SSS, "Mechanical and Thermal Properties of Hierarchical Composites Enhanced by Pristine Graphene and Graphene Oxide Nanoinclusions." *J. Appl. Polym. Sci.*, **131** 40826–40834 (2014)
12. Chang, KC, Hsu, MH, Lu, HI, Lai, MC, Liu, PJ, Hsu, CH, Ji, WF, Chuang, TL, Wei, Y, Yeh, JM, Liu, WR, "Room-Temperature Cured Hydrophobic Epoxy/Graphene Composites as Corrosion Inhibitor for Cold-Rolled Steel." *Carbon*, **66** 144–153 (2014)
13. Chang, KC, Ji, WF, Lai, MC, Hsiao, YR, Hsu, CH, Chuang, TL, Wei, Y, Yeh, JM, Liu, WR, "Synergistic Effects of Hydrophobicity and Gas Barrier Properties on the Anticorrosion Property of PMMA Nanocomposite Coatings Embedded with Graphene Nanosheets." *Polym. Chem. (UK)*, **5** 1049–1056 (2014)
14. Liu, D, Zhao, W, Liu, S, Cen, Q, Xue, Q, "Comparative Tribological and Corrosion Resistance Properties of Epoxy Composite Coatings Reinforced with Functionalized Fullerene C60 and Graphene." *Surf. Coat. Technol.*, **286** 354–364 (2016)
15. Liu, S, Gu, L, Zhao, H, Chen, J, Yu, H, "Corrosion Resistance of Graphene-Reinforced Waterborne Epoxy Coatings." *J. Mater. Sci. Technol.*, **32** 425–431 (2016)
16. Rajabi, M, Rashed, GR, Zaarei, D, "Assessment of Graphene Oxide/Epoxy Nanocomposite as Corrosion Resistance Coating on Carbon Steel." *Corros. Eng. Sci. Technol.*, **50** 509–516 (2015)
17. Ramezanzadeh, B, Niroumandrad, S, Ahmadi, A, Mahdavian, M, Moghadam, MHM, "Enhancement of Barrier and Corrosion Protection Performance of an Epoxy Coating Through Wet Transfer of Amino Functionalized Graphene Oxide." *Corros. Sci.*, **103** 283–304 (2016)
18. Ramezanzadeh, B, Ahmadi, A, Mahdavian, M, "Enhancement of the Corrosion Protection Performance and Cathodic Delamination Resistance of Epoxy Coating Through Treatment of Steel Substrate by a Novel Nanometric Sol-Gel Based Silane Composite Film Filled with Functionalized Graphene Oxide Nanosheets." *Corros. Sci.*, **109** 182–205 (2016)
19. Yu, Z, Di, H, Ma, Y, He, Y, Liang, L, Lv, L, Ran, X, Pan, Y, Luo, Z, "Preparation of Graphene Oxide Modified by Titanium Dioxide to Enhance the Anti-corrosion Performance of Epoxy Coatings." *Surf. Coat. Technol.*, **276** 471–478 (2015)
20. Yu, Z, Lv, L, Ma, Y, Di, H, He, Y, "Covalent Modification of Graphene Oxide by Metronidazole for Reinforced Anti-Corrosion Properties of Epoxy Coatings." *RSC Adv.*, **6** 18217–18226 (2016)
21. Xiao, W, Liu, Y, Guo, S, "Composites of Graphene Oxide and Epoxy Resin Assuming a Uniform 3D Graphene Oxide Network Structure." *RSC Adv.*, **6** 86904–86908 (2016)
22. Yousefi, N, Lin, X, Zheng, Q, Shen, X, Pothnis, JR, Jia, J, Zussman, E, Kim, JK, "Simultaneous In Situ Reduction, Self-Alignment and Covalent Bonding in Graphene Oxide/Epoxy Composites." *Carbon*, **59** 406–417 (2013)
23. Gu, L, Liu, S, Zhao, H, Yu, H, "Facile Preparation of Water-Dispersible Graphene Sheets Stabilized by Carboxylated Oligoanilines and Their Anticorrosion Coatings." *ACS Appl. Mater. Interfaces*, **7** 17641–17648 (2015)
24. Monetta, T, Acquesta, A, Bellucci, F, "Graphene/Epoxy Coating as Multifunctional Material for Aircraft Structures." *Aerospace*, **2** 423–434 (2015)
25. C.D. 1999/13/EC, Official Journal of the European Communities L 85/1–22 (1999)
26. Andreatta, F, Bortolotto, M, Lanzutti, A, Paussa, L, Bravin, D, Fedrizzi, L, "Environmentally friendly conversion coating for aluminium alloy AA6014." *18th International Corrosion Congress*, Perth, Australia, 2011

27. Deflorian, F, Rossi, S, Fedel, M, "Aluminium Components for Marine Applications Protected Against Corrosion by Organic Coating Cycles with Low Environmental Impact." *Corros. Eng. Sci. Technol.*, **46** 237–244 (2011)
28. Sinagra, C, Bravaccino, F, Bitondo, C, Bossio, A, Monetta, T, Mitton, DB, Bellucci, F, "Green Technology for Surface Treatments of Aluminium Foil For Flexible Packaging." *Key Eng. Mater.*, **710** 186–191 (2016)
29. Carangelo, A, Curioni, M, Acquesta, A, Monetta, T, Bellucci, F, "Cerium-Based Sealing of Anodic Films on AA2024T3: Effect of Pore Morphology on Anticorrosion Performance." *J. Electrochem. Soc.*, **163** C907–C916 (2016)
30. Carangelo, A, Curioni, M, Acquesta, A, Monetta, T, Bellucci, F, "Application of EIS to In Situ Characterization of Hydrothermal Sealing of Anodized Aluminum Alloys: Comparison Between Hexavalent Chromium-Based Sealing, Hot Water Sealing and Cerium-Based Sealing." *J. Electrochem. Soc.*, **163** C619–C626 (2016)
31. Carneiro, J, Tedim, J, Fernandes, SCM, Freire, CSR, Silvestre, AJD, Gandini, A, Ferreira, MGS, Zheludkevich, ML, "Chitosan-Based Self-Healing Protective Coatings Doped with Cerium Nitrate for Corrosion Protection of Aluminum Alloy 2024." *Prog. Org. Coat.*, **75** 8–13 (2012)
32. Fetouh, HA, Abdel-Fattah, TM, El-Tantawy, MS, "Novel Plant Extracts as Green Corrosion Inhibitors for 7075-T6 Aluminium Alloy in an Aqueous Medium." *Int. J. Electrochem. Sci.*, **9** 1565–1582 (2014)
33. Gobara, M, Kamel, H, Akid, R, Baraka, A, "Corrosion Behaviour of AA2024 Coated with an Acid-Soluble Collagen/Hybrid Silica Sol–Gel Matrix." *Prog. Org. Coat.*, **89** 57–66 (2015)
34. Monetta, T, Acquesta, A, Maresca, V, Signore, R, Bellucci, F, Di Petta, P, Lo Masti, M, "Characterization of Aluminum Alloys Environmentally Friendly Surface Treatments for Aircraft and Aerospace Industry." *Surf. Interface Anal.*, **45** 1522–1529 (2013)
35. Bitondo, C, Bossio, A, Monetta, T, Curioni, M, Bellucci, F, "The Effect of Annealing on the Corrosion Behaviour of 444 Stainless Steel for Drinking Water Applications." *Corros. Sci.*, **87** 6–10 (2014)
36. Monetta, T, Mitton, DB, Bellucci, F, "Protective Properties of Organic Coatings on Plasma-Treated Cold Rolled Aluminum." *Electrochem. Solid State Lett.*, **7** B39–B41 (2004)
37. De Rosa, L, Monetta, T, Bellucci, F, "Moisture Uptake in Organic Coatings Monitored with EIS." *Mater. Sci. Forum*, **289–292** 315–326 (1998)
38. Mansfeld, F, "Use of Electrochemical Impedance Spectroscopy for the Study of Corrosion Protection by Polymer Coatings." *J. Appl. Electrochem.*, **25** 187–202 (1995)
39. Bellucci, F, Nicodemo, L, "Water Transport in Organic Coatings." *Corrosion*, **49** 235–247 (1993)
40. Nicodemo, L, Bellucci, F, Marcone, A, Monetta, T, "Water and Oxygen Transport as Performance Parameters of Paint Films." *J. Membr. Sci.*, **52** 393–403 (1990)
41. Walter, GW, "A Review of Impedance Plot Methods Used for Corrosion Performance Analysis of Painted Metals." *Corros. Sci.*, **26** 681–703 (1986)
42. Ku, CC, Liepins, R, *Appendix 1 in Electrical Properties of Polymers: Chemical Principles*, pp. 334–345. Hanser Publishers, Munich (1987)
43. Su, Y, Kravets, VG, Wong, SL, Waters, J, Geim, AK, Nair, RR, "Impermeable Barrier Films and Protective Coatings Based on Reduced Graphene Oxide." *Nat. Commun.*, **5** 4843–4847 (2014)
44. Yoo, BM, Shin, HJ, Yoon, HW, Park, HB, "Graphene and Graphene Oxide and Their Uses in Barrier Polymers." *J. Appl. Polym. Sci.*, **131** 39628–39651 (2014)